Monatshefte für Chemie 130, 1179–1193 (1999)

Monatshefte für Chemie
Chemical Monthly

Thermal Behaviour and Crystal Structure of Sodium-Containing Hemihydrates of Calcium Sulfate

Daniela Freyer[1], **Günter Reck**[2], **Martina Bremer**[1], and **Wolfgang Voigt**[1,*]

[1] TU Bergakademie Freiberg, Institut für Anorganische Chemie, D-09596 Freiberg, Germany
[2] Bundesanstalt für Materialforschung und -prüfung, D-12489 Berlin, Germany

Summary. A metastable sodium-containing hemihydrate ($(6\text{-}x)CaSO_4 \cdot xNa_2SO_4 \cdot 3H_2O$, $0 \leq x \leq 1$) limited by the pentasalt composition $Na_2SO_4 \cdot 5CaSO_4 \cdot 3H_2O$ occurs as an intermediate solid phase in the systems Na_2SO_4-$CaSO_4$-H_2O, NaCl-Na_2SO_4-$CaSO_4$-H_2O, and NaCl-$CaSO_4$-H_2O. X-Ray structure determination of a crystal with pentasalt composition results in a super-structure of the pure hemihydrate ($CaSO_4 \cdot 0.5H_2O$), in which one Ca^{2+}ion is statistically replaced by two Na^+ ions. One Na^+ cation is situated in a Ca^{2+} position in only one of the three chains of $CaSO_4$ forming an axis of nearly three fold symmetry along the *c*-axis. The second Na^+ is located in the water channel neighbouring to the first Na^+. The hydrate crystallized in a monoclinic space group C121 (No. 5) with $a = 24.1781(11)$, $b = 13.805(2)$, $c = 12.7074(12)$ Å, $\beta = 90.089(12)°$. The dehydration temperature of the hydrates depends on their Na^+ ion content. A high Na^+ content (in water channels) blocks the water escape strongly, and the dehydration temperature increases. Thermal behaviour is also effected by the crystal sizes. The thermograms of small crystals as opposed to large ones show a exothermic effect adjoining the endothermic dehydration. This may be indicative for a change in the dehydration mechanism upon crystal size.

Keywords. Bassanite; Crystal structure; Sodium pentasalt; Calcium sulfate hemihydrate; Thermal analysis.

Thermisches Verhalten und Struktur von natriumhaltigen Calciumsulfathemihydraten

Zusammenfassung. Ein metastabiles natriumhaltiges Calciumsulfathemihydrat ($(6-x)CaSO_4 \cdot xNa_2SO_4 \cdot 3H_2O$, $0 \leq x \leq 1$) tritt als intermediäre Phase in den Systemen Na_2SO_4-$CaSO_4$-H_2O, NaCl-Na_2SO_4-$CaSO_4$-H_2O und NaCl-$CaSO_4$-H_2O auf. Die Phase mit dem höchsten Natriumionengehalt entspricht dem sogenannten Natriumpentasalz ($Na_2SO_4 \cdot 5CaSO_4 \cdot 3H_2O$). Die Röntgenstrukturanalyse, welche an einem Einkristall mit Pentasalz-Zusammensetzung durchgeführt wurde, ergab eine Überstruktur des reinen Hemihydrats ($CaSO_4 \cdot 0.5H_2O$), wobei ein Ca^{2+}-Ion statistisch durch zwei Na^+-Ionen ersetzt ist. Die Ca^{2+}-Substitution erfolgt nur in einer der drei $CaSO_4$-Ketten, welche eine nahezu dreizählige Achse entlang der *c*-Achse bilden. Ein Ca^{2+}-Ion wird durch ein Na^+-Ion ersetzt, das zweite Na^+-Ion ist in unmittelbarer Nähe zum ersten in den Wasserkanälen eingelagert. Das Hydrat kristallisiert in der monoklinen Raumgruppe C121 (Nr.5) mit den Gitterparametern $a = 24.178(11)$, $b = 13.805(2)$, $c = 12.7074(12)$ Å, $\beta = 90.089(12)°$. Die

* Corresponding author

Dehydratationstemperatur variiert mit dem Na^+-Gehalt. Je größer dieser ist, um so stärker wird der Austritt der H_2O-Moleküle blockiert und zu höheren Temperaturen verschoben. Ein weiterer Unterschied im thermischen Verhalten wurde bei gleichem Na^+-Gehalt für unterschiedliche Kristallitgrößen gefunden. Bei kleinen Kristallgrößen (Nadellänge < 20 µm) beginnt die Entwässerung früher im Vergleich zu größeren Kristallen (Nadellänge > 50 µm). Ein exothermer Effekt im Anschluß an die Dehydratation wird nur für kleine Kristalle beobachtet und deutet auf eine abweichende Entwässerungskinetik in Abhänigkeit von der Kristallitgröße hin.

Introduction

In connection with our studies on the formation of anhydrous and hydrated $Na_2SO_4/CaSO_4$ phases [1, 2] we became interested in the nature of the double salt $Na_2SO_4 \cdot 5CaSO_4 \cdot 3H_2O$, the so-called 'pentasalt'. This phase is reported as a stoichiometric metastable solid which occurs during conversion of gypsum into glauberite ($Na_2SO_4 \cdot CaSO_4$) or anhydrite ($CaSO_4$) in solutions of the systems Na_2SO_4-$CaSO_4$-H_2O [3–5] or NaCl-Na_2SO_4-$CaSO_4$-H_2O [6] at temperatures between 50 and 85°C. The molar H_2O/SO_4 ratio in the pentasalt is the same as in the mineral bassanite ($CaSO_4 \cdot 0.5H_2O$). The X-Ray powder diffraction pattern resembles that of bassanite except for splitting of many reflections. This similarity can be explained by analogous crystal structures with 1/6 of the Ca^{2+} ions being statistically substituted by Na^+ ions [7]. Charge neutrality is reached by a second Na^+ ion located in the water channel along the *c*-axis of the bassanite structure. This substitution scheme yields the stoichiometry $Na_2SO_4 \cdot 5CaSO_4 \cdot 3H_2O$ or $(Ca_{0.83}Na_{0.33})SO_4 \cdot 0.5H_2O$ as one possibility. The statistical substitution should result in variable sodium content in dependence on the Na^+ concentration of the solution from which the salt is crystallized. However, pentasalt has always been reported with fixed stoichiometry, although it was formed or equilibrated in solutions with 0.5–3.0 mol Na_2SO_4/kg H_2O.

For a sodium containing calcium sulfate hemihydrate, $(Ca_{0.98}Na_{0.03})SO_4 \cdot 0.47H_2O$ obtained from a saturated NaCl solution, a similar structure model has been discussed [8, 9]. The authors emphasize that the product was free of Cl^-. In comparison to the sodium-free hemihydrate, the *X*-ray powder diagram showed splitting of reflexes (analogous to the pentasalt) and had to be indexed with an increased monoclinic angle γ of 90.27° compared with 90.0° for the Na^+-free salt [9]. The pentasalt is found to be triclinic with all angles slightly above 90° [7]. In both cases the lattice parameters are nearly identical with the Na^+-free hemihydrate (pentasalt, $Na_2SO_4 \cdot 5CaSO_4 \cdot 3H_2O$ [7]: $a = 6.898$, $b = 12.076$, $c = 12.706$ Å; $(Ca_{0.98}Na_{0.03})SO_4 \cdot 0.47H_2O$ [9]: $a = 12.107$, $b = 12.718$, $c = 6.910$ Å; hemihydrate [10]: $a = 12.019$, $b = 6.930$, $c = 12.670$ Å; $\beta = 90.2°$). This situation encouraged us to check whether the stoichiometry is variable or not and to try to isolate single crystals of pentasalt for crystal structure analysis which is not available until now.

Results and Discussion

Synthesis

Gypsum or hemihydrate was suspended in different solutions at 60–75°C for 20 h up to one week. Products of varying sodium content have been obtained as given in

Table 1. Compositions of hydrates synthesized from $CaSO_4$ hydrate phases in various solutions

	Chemical composition of hydrate	Solution system	Initial $CaSO_4$ hydrate phase
1	$6CaSO_4 \cdot 2.90H_2O$	HNO_3-H_2O	$CaSO_4 \cdot 2H_2O$
2	$0.23Na_2SO_4 \cdot 5.77CaSO_4 \cdot 2.95H_2O$	NaCl-H_2O	$CaSO_4 \cdot 0.5H_2O$
3	$0.90Na_2SO_4 \cdot 5.10CaSO_4 \cdot 2.85H_2O$	NaCl-H_2O	$CaSO_4 \cdot 2H_2O$
4	$0.94Na_2SO_4 \cdot 5.06CaSO_4 \cdot 2.98H_2O$	NaCl-Na_2SO_4-H_2O	$CaSO_4 \cdot 2H_2O$
5	$1.01Na_2SO_4 \cdot 4.99CaSO_4 \cdot 2.90H_2O$	Na_2SO_4-H_2O	$CaSO_4 \cdot 2H_2O$
6	$1.01Na_2SO_4 \cdot 4.99CaSO_4 \cdot 2.86H_2O$	NaCl-Na_2SO_4-H_2O	$CaSO_4 \cdot 2H_2O$

Table 1. The empirical formulas in Table 1 are related to six mol SO_4^{2-} to facilitate comparisons with the ideal pentasalt formula.

It can be seen that the water content remains constant at 2.92 ± 0.07 mol that is converted near the hemihydrate (0.487 ± 0.01). The use of hemihydrate as starting material yields a lower Na_2SO_4 content at comparable preparation conditions (**2**, **3**). $Na_2SO_4 \cdot 5CaSO_4 \cdot 3H_2O$ represents obviously a limiting composition which can be obtained reproducible (**5**, **6**).

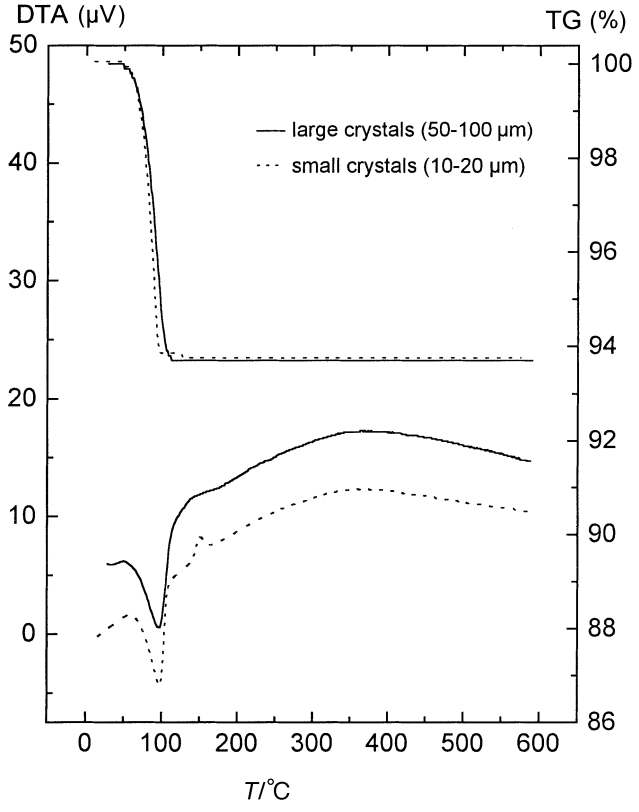

Fig. 1. Thermal behaviour of sample **1**: $6CaSO_4 \cdot 2.90H_2O$ (large- and small-sized α-form crystals)

Thermal behaviour

At first the thermal behaviour of the sodium-free hemihydrate will be discussed. From literature it is known that, depending on the preparation procedure, a well-crystallized α-form and a poorly crystallized β-form can be obtained which differ in their thermal behaviour and other properties [11–16]. The TG curves of α- and β-$CaSO_4 \cdot 0.5H_2O$ are identical when using the same heating rates. The course of the DTA curves allows to distinguish between α- and β-form. α-$CaSO_4 \cdot 0.5H_2O$ gives an exothermic effect which closely follows the endothermic dehydration effect at 217°C. The exothermic effect of β-$CaSO_4 \cdot 0.5H_2O$ is much broader and can be observed between 320°C and 375°C. Both effects are attributed to the lattice conversion from the hexagonal (AIII) to orthorhombic form (AII). The differences observed in the exothermic effects are possibly associated with the dehydration kinetics dependent on surface area, porosity, crystallinity, *etc.* [11, 15, 16]. Opposite to these observations, *Budnikov* and *Kosyreva* [17] have claimed that the thermogram of the α-form does not exhibit an exothermic effect.

We could always reproduce the thermal behaviour of the α-form prepared from solution as can be seen from Fig. 1. However, we found also a difference in the exothermic effect depending on the crystal size of the α-form. The hemihydrate forms needle-like crystals; at a needle length between 10 and 20 µm the exothermic effect is clearly visible but disappears at lengths of approximately 50–100 µm.

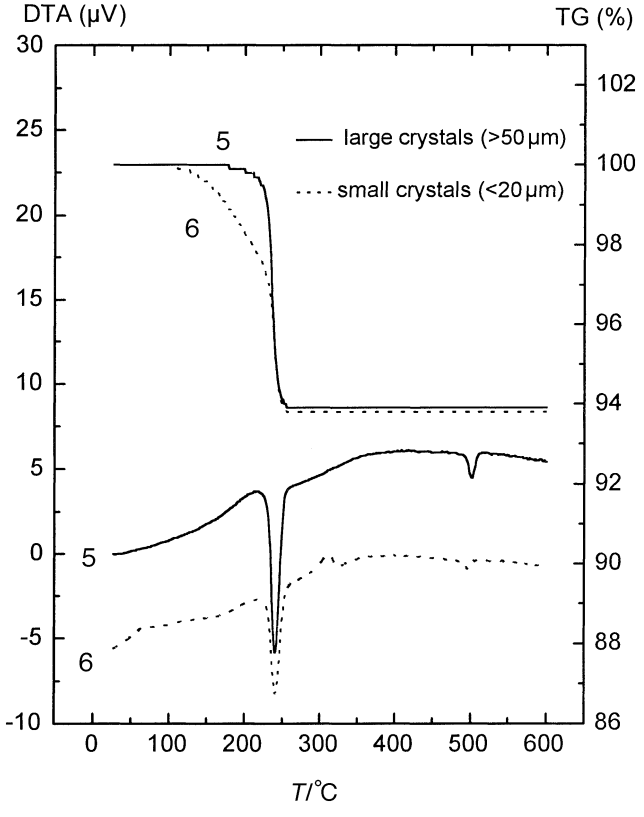

Fig. 2. Thermal behaviour of sample **5**; $1.01Na_2SO_4 \cdot 4.99CaSO_4 \cdot 2.90H_2O$ (large-sized crystals) and sample **6**: $1.01Na_2SO_4 \cdot 4.99CaSO_4 \cdot 2.86H_2O$ (small-sized crystals)

Large crystals (50–100 µm) were prepared at conditions of reduced mixing intensity, reduced suspension density, and constant temperature ($\Delta T < \pm 0.5°C$). From NaCl solution, also under these conditions only small-sized crystals could be prepared. This result explains why an exothermic effect for the α-$CaSO_4 \cdot 0.5H_2O$ has not been observed so far by different authors.

Figure 2 shows the thermal behaviour of samples **5** and **6** with pentasalt composition. In agreement with literature [4, 6, 7], two endothermic effects are observed at 225–235°C and 500–520°C. The first one corresponds to the dehydration and simultaneous formation of anhydrite ($CaSO_4$) and glauberite ($Na_2SO_4 \cdot CaSO_4$). At 500–520°C glauberite is decomposed. Interestingly, in the DTA curve of sample **6** after dehydration an exothermic effect occurs analogous to the small crystallite α-form of $CaSO_4 \cdot 0.5H_2O$. Dehydration begins at a lower temperature for sample **6** than for sample **5**.

Since the exothermic effect is shifted towards higher temperatures by approximately 150 K, it cannot be due to the presence of sodium-free hemihydrate.

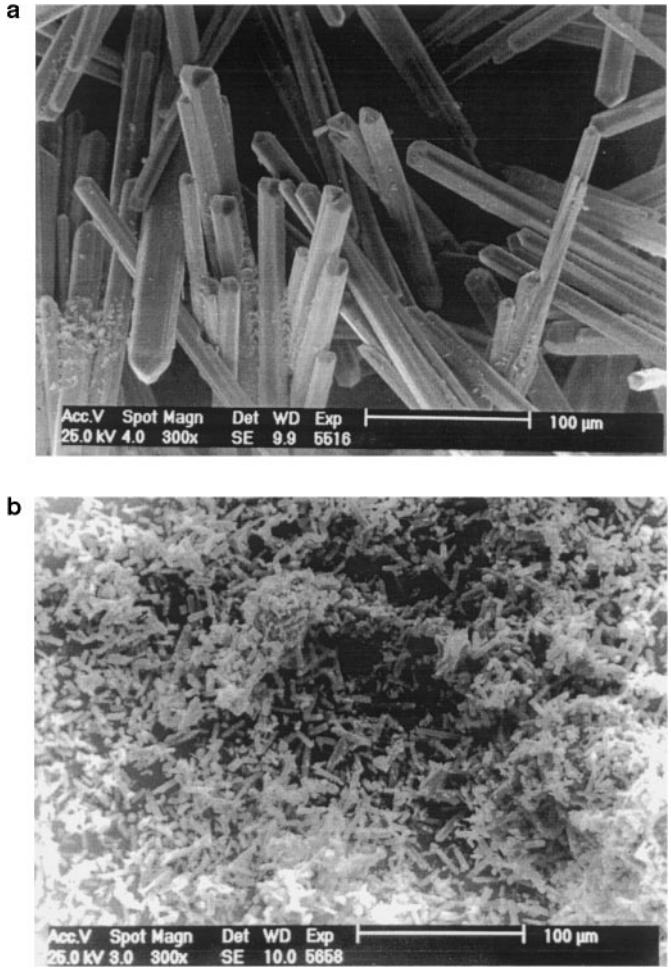

Fig. 3. SEM photographs for (a) sample **5**: $1.01Na_2SO_4 \cdot 4.99CaSO_4 \cdot 2.90H_2O$ (large-sized crystals) and (b) sample **4**: $1.01Na_2SO_4 \cdot 4.99CaSO_4 \cdot 2.86H_2O$ (small-sized crystals)

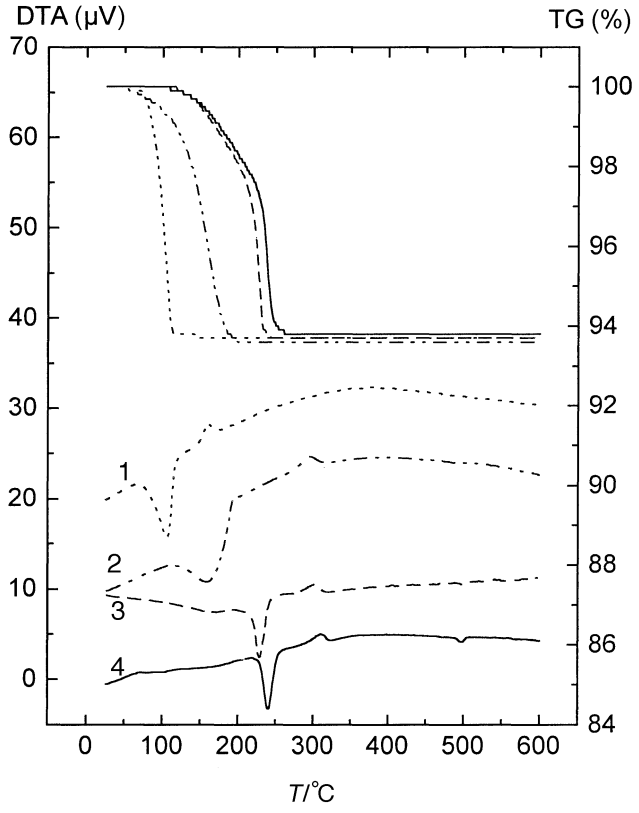

Fig. 4. Comparison of the thermal behaviour of the hydrates; **1**: $6CaSO_4 \cdot 2.90H_2O$, **2**: $0.23Na_2SO_4 \cdot 5.77CaSO_4 \cdot 2.95H_2O$, **3**: $0.90Na_2SO_4 \cdot 5.10CaSO_4 \cdot 2.85H_2O$, **6**: $1.01Na_2SO_4 \cdot 4.99CaSO_4 \cdot 2.86H_2O$ (all small-sized crystals)

A comparison of the crystal size gave a result similar to the α-form $CaSO_4 \cdot 0.5H_2O$ crystals. This view is supported by the SEM photographs shown in Fig. 3. Crystal sizes in sample **5** (> 50 μm) are much larger than in **6** (10–20 μm). For the pentasalt the exothermic effect at 310°C becomes invisible at needle lengths above 50 μm.

The dependence of the thermal behaviour on the sodium content is shown in Fig. 4. The small-sized crystals were selected for all samples, because until now we were not successful in preparing large-sized crystals with intermediate sodium content from NaCl containing systems. The curves clearly reflect a continuous increase of the temperature of dehydration with increasing content of Na_2SO_4. This gives an indication that the samples could be considered as a solid solution series, but we were not successful in preparation of a complete series with varying Na_2SO_4 content.

X-Ray powder diffraction and structure description

X-Ray powder diagrams of the samples show peak broadening with increasing Na_2SO_4 content (Fig. 5). At the pentasalt composition, distinct splitting of peaks and appearance of weak new reflections is observed as demonstrated in Fig. 6. The

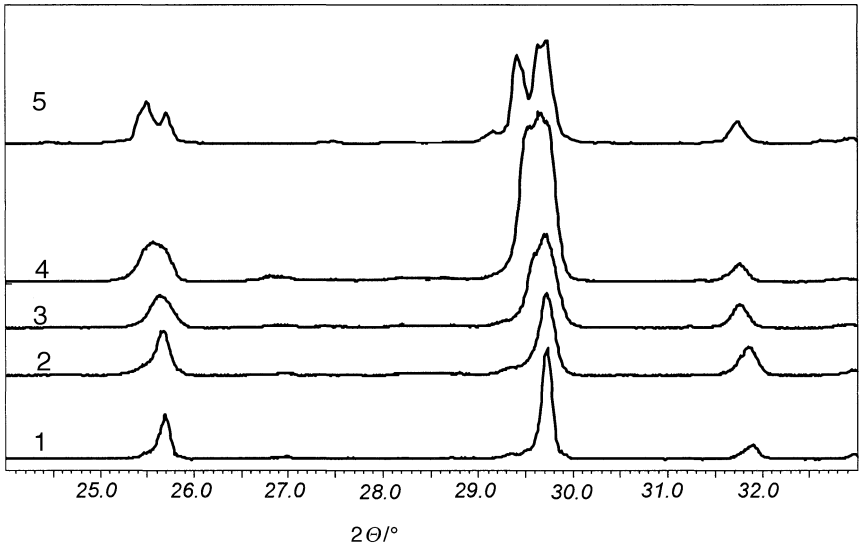

Fig. 5. Powder diffractograms of the hydrates; **1**: $6CaSO_4 \cdot 2.90H_2O$, **2**: $0.23Na_2SO_4 \cdot 5.77CaSO_4 \cdot 2.95H_2O$, **3**: $0.90Na_2SO_4 \cdot 5.10CaSO_4 \cdot 2.85H_2O$, **4**: $0.94Na_2SO_4 \cdot 5.06CaSO_4 \cdot 2.98H_2O$, **5**: $1.01Na_2SO_4 \cdot 4.99CaSO_4 \cdot 2.90H_2O$

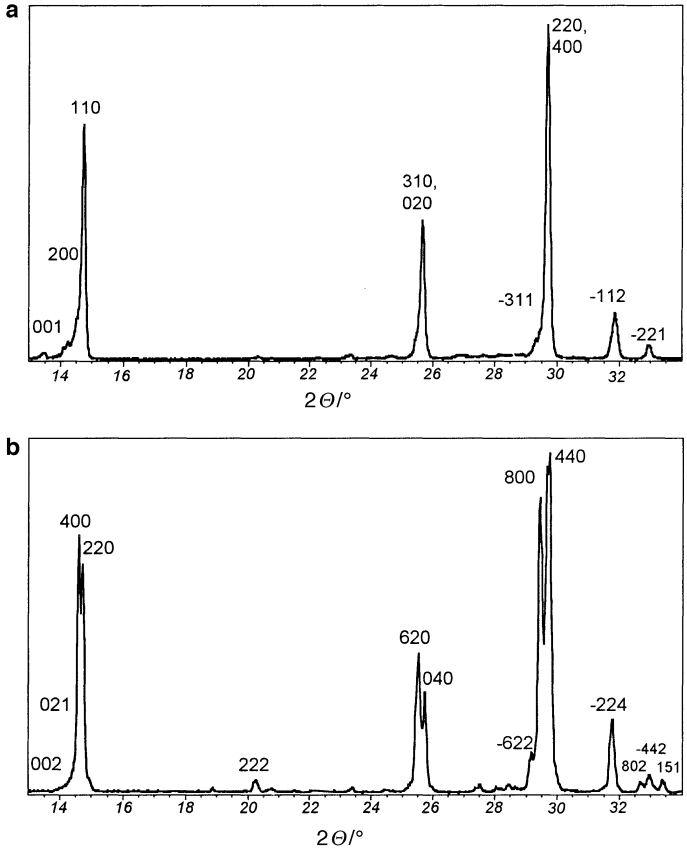

Fig. 6. Powder diffractograms of samples **1** ($6CaSO_4 \cdot 2.90H_2O$, a) and **5** ($1.01Na_2SO_4 \cdot 4.99CaSO_4 \cdot 2.90H_2O$, b)

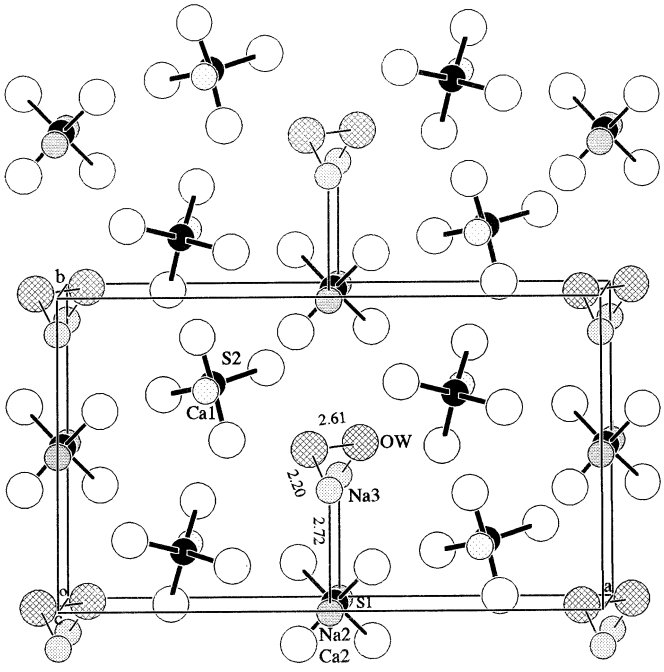

Fig. 7. Representation of the crystal structure with atoms in the sub-cell along the *c*-axis

complete pattern agrees with PDF 40-718 [7] and also with PDF 37-246 [9]. Small- and large-sized crystals yield identical powder diagrams.

From crystal structure analysis it follows that the composition $Na_2SO_4 \cdot 5CaSO_4 \cdot 3H_2O$ represents a maximum degree of Ca^{2+}-Na^+ substitution in the hemihydrate. Figure 7 shows the starting model with an arrangement of atoms in the superposition structure neglecting Na atoms similar to that of bassanite (or hemihydrate). The sodium-free unit cell contains 6 formula units hemihydrate with 4 Ca(1) and 2 Ca(2) atoms [10]. The three water molecules are statistically distributed on 4 crystallographic sites within channels.

Only the Ca(2) atoms are partly replaced by Na atoms. The second Na atom, necessary for charge neutrality, was found within the channels in a special position on a two-fold axis of the space group. Thus, at maximum half of the Ca(2) can be substituted. This gives the limiting formula $Na_2SO_4 \cdot 5CaSO_4 \cdot 3H_2O$. Distances between Na(3) (in the channel) and Na(2) (on Ca(2) position) as well as Na(3) and O(water) in the superposition structure amount of 2.72 and 2.20 Å, respectively. Especially the Na-Na distance is too short. It should not be considerably smaller than 3.2 Å. Therefore, progressive substitution of Ca(2) gives rise to distortions. This causes a symmetry decrease and the subsequent formation of a super-structure (Fig. 8) with doubling of *a*, *b*, and *c* lattice constants and an increased monoclinic angle. The refinement of the super-structure gave acceptable values for all Na-Na distances. Using the determined structural parameters, a theoretical powder diffractogramm was calculated which is in good agreement with the experimental powder pattern.

In view of the gradual change of thermal and structural properties, the sodium containing hydrates should be considered as a solid solution series with the end

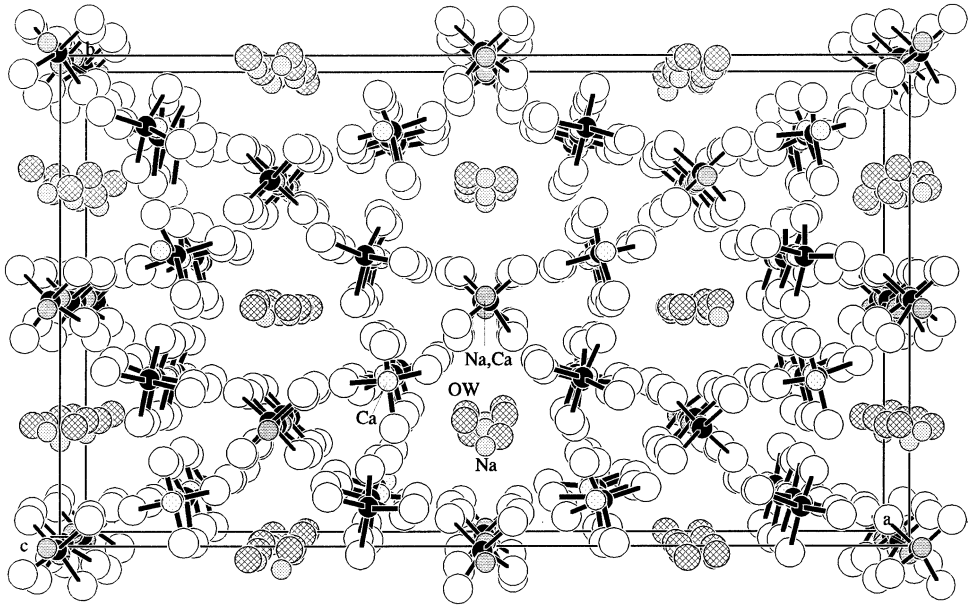

Fig. 8. Representation of the crystal structure using atoms in the super-structure along the *c*-axis

members $6CaSO_4 \cdot 3H_2O$ and $Na_2SO_4 \cdot 5CaSO_4 \cdot 3H_2O$. However, detailed investigations about continuity of the solid solutions, ordering effects, and other phenomena require more efforts in the preparation of samples with varying sodium content.

Experimental

$CaSO_4 \cdot 0.5H_2O$

Gypsum (25 g, $CaSO_4 \cdot 2H_2O$, Merck) was stirred at 60±2°C in 200 cm^3 conc. HNO_3 for 24 h. In order to obtain large-sized crystals, the suspension density was lowered to 5 g gypsum in the same volume of acid, and temperature variations were reduced to ±0.5 K.

$5.77CaSO_4 \cdot 0.23Na_2SO_4 \cdot 2.95H_2O$ (small-sized crystals)

$CaSO_4 \cdot 0.5H_2O$ (20 g) was stirred in 250 cm^3 saturated NaCl solution for 24 h at 70±2°C.

$5.10CaSO_4 \cdot 0.90Na_2SO_4 \cdot 2.85H_2O$ (small-sized crystals)

Gypsum (15 g, Merck) was stirred in 200 cm^3 saturated NaCl solution for 20 h at 70±2°C.

$5.06CaSO_4 \cdot 0.95Na_2SO_4 \cdot 2.98H_2O$ (small-sized crystals)

Gypsum (2 g, Merck) and 0.25 g Na_2SO_4 (Merck) were stirred in 20 g saturated NaCl solution for one week at 75±0.5°C.

$4.99CaSO_4 \cdot 1.01Na_2SO_4 \cdot 2.90H_2O$ (large-sized crystals)

Prepared from 2 g gypsum (Merck), 3.336 g Na_2SO_4 (Merck), and 20 g H_2O for one week at 75±0.5°C.

$4.99CaSO_4 \cdot 1.01Na_2SO_4 \cdot 2.86H_2O$ (small-sized crystals)

Gypsum (2 g, Merck) and 0.515 g Na_2SO_4 (Merck) were agitated in 20 g saturated NaCl solution for one week at 75±0.5°C.

All hydrates were separated from the mother liquor at the temperature of the synthesis. Subsequently, the phases were washed with a mixture of cold water and ethanol (70:30) and dried at 60°C for one day.

For all prepared hydrates chemical analyses were performed. The NaCl content from adherent mother liquor was determined by potentiometric titration of chloride. By complexometric titration with calcon carbon acid the Ca^{2+} content in the samples was obtained. Additionally, the $CaSO_4$ content in a much larger sample **2** was determined by extraction of Na_2SO_4 in aqueous solution. The residue of gypsum was dehydrated at 300°C for 5 h and weighted. The $CaSO_4$ content (corrected by the gypsum solubility in water) found in this way agrees within ±0.05 mol $CaSO_4$ with the complexometric result. The hydrate water were determined thermogravimetrically.

TG/DTA measurements were carried out in nitrogen (300 cm^3/min) at 5 K/min from room temperature up to 600°C using a DTA/TA 22 (Seiko).

The powder diffraction patterns were recorded with a D 5000 powder diffractometer (Siemens) using CuK_α radiation. Standard: silicon; counting time: 10s; step size: 0.01°.

X-Ray structure determination

For the structure determination, crystals from large-size pentasalt samples were used. Unfortunately, only an extremely small twinned crystal of dimensions 0.12×0.02×0.02 mm was available. Nevertheless, after an extremely long exposure time a complete intensity data set could be collected on a *Bruker AXS SMART* diffractometer with a CCD area detector. The structure refinement gave an

Table 2. Crystal data and structure refinement for $Ca_{0.86}Na_{0.28}SO_4 \cdot 0.48H_2O$ (sub-cell)

Empirical formula	$H_{1.42}Ca_{1.29}Na_{0.43}O_{6.71}S_{1.50}$
Formula weight	218.26
Temperature	293 (2) K
Wavelength	0.71073 (Å)
Crystal system, space group	monoclinic, C2 (No. 5)
Unit cell dimensions	$a = 12.0890$ (11) Å
	$b = 6.903$ (2) Å
	$c = 6.3537$ (12) Å
	$\beta = 90.089$ (12)°
Volume	530.2 (2)Å^3
Z, Calculated density	4,2.734 Mg/m^3
Absorption coefficient	2.056 mm^{-1}
F (000)	438
Crystal size	0.12×0.02×0.02 mm
Θ range for data collection	3.21 to 23.42 deg.
Index ranges	$-12 \le h \le 13$, $-7 \le k \le 7$, $-7 \le l \le 7$
Reflections collected/unique	1237/670 (R(int) = 0.0987)
Refinement method	Full-matrix least-squares on F^2
Data/restraints/parameters	670/2/104
Final R indices ($I > 2\sigma(I)$)	$R_1 = 0.0938$, $wR_2 = 0.2363$
R indices (all data)	$R_1 = 0.0970$, $wR_2 = 0.2406$
Extinction coefficient	0.002 (4)
Largest diff. peak and hole	0.990 and −0.504 e · A^{-3}

Table 3. Atomic coordinates ($\cdot 10^{-4}$) and equivalent isotropic displacement parameters ($Å^{-2} \cdot 10^{-3}$) for $Ca_{0.86}Na_{0.28}SO_4 \cdot 0.48H_2O$ (sub-cell)

	Wyck	*x*	*y*	*z*	*U*(eq)	SOF
S (1)	2b	0	40(5)	5000	19(1)	
S (2)	4c	2726(2)	1842(3)	1690(3)	17(1)	
Ca (1)	4c	2685(2)	1884(3)	6671(3)	33(1)	
Ca (2)	2a	0	−66(6)	0	21(1)	0.572(10)
Na (2)	2a	0	−66(6)	0	21(2)	0.428(19)
O (1)	4c	710(6)	1244 (11)	6354(12)	37(2)	
O (2)	4c	1782(6)	1464(16)	203(11)	43(2)	
O (3)	4c	3691(6)	2302(14)	422(14)	41(2)	
O (4)	4c	2453(8)	3417(11)	3020(11)	42(2)	
O (5)	4c	2988(7)	143(12)	2934(12)	34(2)	
O (6)	4c	655(6)	−1235(13)	3584(10)	34(2)	
O (1W)	4c	430(15)	5030(3)	3120(4)	119(9)	0.71(3)
Na (3)	2a	0	3880(5)	0	100(10)	0.428(19)

Table 4. Crystal data and structure refinement for $Ca_{0.86}Na_{0.28}SO_4 \cdot 0.48H_2O$ (super-structure)

Empirical formula	$H_{11.56}Ca_{10.29}Na_{3.42}O_{53.78}S_{12}$
Formula weight	1747.91
Temperature	293 (2) K
Wavelength	0.71073 (Å)
Crystal system, space group	monoclinic, C2 (No. 5)
Unit cell dimensions	$a = 24.1781$ (11) Å $b = 13.805$ (2) Å $c = 12.7074$ (12) Å $\beta = 90.089$ (12)°
Volume	4241.6 (8)Å^3
Z, Calculated density	4, 2.737 Mg/m^3
Absorption coefficient	2.057 mm^{-1}
F (000)	3509
Crystal size	0.12×0.02×0.02 mm
Θ range for data collection	1.60 to 23.70 deg.
Index ranges	$-20 \le h \le 26$, $-15 \le k \le 15$, $-14 \le l \le 14$
Reflections collected/unique	8292/5451 (R(int) = 0.1449)
Absorptions correction	none
Refinement method	Full-matrix least-squares on F^2
Data/restraints/parameters	5451/3706/781
Final *R* indices ($I > 2\sigma(I)$)	$R_1 = 0.1387$, $wR_2 = 0.3332$
R indices (all data)	$R_1 = 0.1867$, $wR_2 = 0.3634$
Extinction coefficient	0.00201 (16)
Largest diff. peak and hole	0.841 and −1.471 e · A^{-3}

empirical formula of $Ca_{0.857}Na_{0.285}SO_4 \cdot 0.482H_2O$ which correspond to $0.86Na_2SO_4 \cdot 5.14CaSO_4 \cdot 2.89H_2O$. Taking into account the relative e.s.d.s of the occupation factors, this is in good agreement with the chemical analysis. Structural parameters as well as details of data collection and structure determination are listed in Tables 2 and 4.

Table 5. Atomic coordinates ($\cdot 10^{-4}$) and equivalent isotropic displacement parameters ($Å^{-2} \cdot 10^{-3}$) for $Ca_{0.86}Na_{0.28}SO_4 \cdot 0.48H_2O$ (super-structure)

	Wyck	*x*	*y*	*z*	*U* (eq)	SOF
S (11)	4c	5029(1)	5017(3)	2474(2)	27(1)	
S (12)	4c	4967(1)	13(3)	2543(2)	26(1)	
S (15)	4c	2500(2)	2572(3)	2505(3)	25(1)	
S (16)	4c	2503(2)	7454(3)	2502(3)	27(1)	
S (21)	4c	1357(2)	966(3)	826(3)	26(1)	
S (22)	4c	1378(2)	5953(3)	832(3)	24(1)	
S (23)	4c	3645(2)	908(3)	4177(3)	26(1)	
S (24)	4c	3620(2)	5899(3)	4164(3)	22(1)	
S (25)	4c	3843(2)	3385(3)	814(3)	31(1)	
S (26)	4c	3888(2)	8440(3)	872(3)	24(1)	
S (27)	4c	1159(1)	3431(2)	4194(3)	13(1)	
S (28)	4c	1123(1)	8464(3)	4134(3)	22(1)	
Ca (11)	4c	1399(2)	987(2)	3338(3)	42(1)	
Ca (12)	4c	1275(2)	6020(3)	3348(3)	52(1)	
Ca (13)	4c	3615(1)	879(2)	1673(3)	29(1)	
Ca (14)	4c	3706(2)	5935(3)	1652(3)	50(1)	
Ca (15)	4c	3867(1)	3413(3)	3341(3)	31(1)	
Ca (16)	4c	3813(2)	8405(3)	3352(3)	44(1)	
Ca (17)	4c	1115(2)	3490(3)	1656(3)	42(1)	
Ca (18)	4c	1198(2)	8499(3)	1628(3)	61(2)	
Ca (21)	2b	5000	89(4)	0	22(2)	0.519(12)
Na (21)	2b	5000	89(4)	0	22(2)	0.48(2)
Ca (22)	2a	5000	−155(4)	5000	37(2)	0.806(12)
Na (22)	2a	5000	−155(4)	5000	37(2)	0.18(3)
Ca (23)	2b	5000	4838(3)	0	26(1)	0.856(12)
Na (23)	2b	5000	4838(3)	0	26(1)	0.15(3)
Ca (24)	2a	5000	5092(4)	5000	10(2)	0.335(11)
Na (24)	2a	5000	5092(4)	5000	10(2)	0.66(2)
Ca (25)	4c	2469(2)	2448(4)	14(4)	21(1)	0.320(5)
Na (25)	4c	2469(2)	2448(4)	14(4)	21(1)	0.693(15)
Ca (26)	4c	2528(2)	2438(4)	4989(3)	33(1)	0.710(9)
Na (26)	4c	2528(2)	2438(4)	4989(3)	33(1)	0.288(18)
Na (31)	2b	5000	7150(15)	0	700(4)	0.15(4)
Na (32)	2a	5000	7341(14)	5000	280(3)	0.66(3)
Na (33)	2b	5000	2380(15)	0	510(8)	0.48(3)
Na (34)	2a	5000	2164(15)	5000	260(4)	0.18(3)
Na (35)	4c	2772(9)	4685(13)	−345(11)	281(17)	0.69(2)
Na (36)	4c	2285(14)	4702(16)	5200(2)	310(4)	0.29(2)
O (11)	4c	5437(3)	5630(6)	3016(7)	52(4)	
O (12)	4c	5313(3)	589(6)	3258(6)	98(4)	
O (13)	4c	4574(3)	645(5)	1970(6)	27(3)	
O (14)	4c	4699(3)	5621(5)	1736(6)	41(3)	
O (15)	4c	2886(3)	3188(5)	3115(6)	24(3)	
O (16)	4c	2841(3)	8061(6)	3233(7)	59(4)	
O (17)	4c	2129(3)	3173(5)	1882(6)	73(3)	
O (18)	4c	2166(3)	8085(5)	1824(7)	151(5)	
O (21)	4c	857(3)	733(8)	209(6)	115(7)	

Table 5 (*continued*)

	Wyck	*x*	*y*	*z*	*U* (eq)	SOF
O (22)	4c	960(3)	5639(7)	53(5)	44(4)	
O (23)	4c	4172(3)	888(8)	4778(6)	70(5)	
O (24)	4c	4068(3)	5753(6)	4945(6)	42(3)	
O (25)	4c	3315(3)	3362(7)	214(6)	44(4)	
O (26)	4c	3426(3)	8314(7)	124(6)	55(4)	
O (27)	4c	1643(3)	3197(7)	4854(6)	74(5)	
O (28)	4c	1539(3)	8123(7)	4889(6)	61(4)	
O (31)	4c	1818(3)	1170(7)	111(6)	58(4)	
O (32)	4c	1889(3)	6237(7)	284(6)	43(4)	
O (33)	4c	3190(3)	1147(8)	4912(6)	69(5)	
O (34)	4c	3123(3)	6248(7)	4719(6)	66(5)	
O (35)	4c	4291(3)	3630(7)	78(6)	52(4)	
O (36)	4c	4387(3)	8778(7)	310(6)	53(4)	
O (37)	4c	684(3)	3611(7)	4901(6)	49(4)	
O (38)	4c	614(3)	8766(6)	4674(6)	56(4)	
O (41)	4c	1251(3)	1781(4)	1523(6)	27(3)	
O (42)	4c	1156(3)	6741(5)	1479(5)	27(3)	
O (43)	4c	3671(5)	1658(5)	3358(5)	140(5)	
O (44)	4c	3791(4)	6605(6)	3370(6)	1136(6)	
O (45)	4c	3807(5)	4118(6)	1642(6)	140(8)	
O (46)	4c	3743(5)	9167(6)	1675(6)	140(8)	
O (47)	4c	1268(3)	4264(4)	3536(6)	41(3)	
O (48)	4c	1339(3)	9259(4)	3489(6)	19(3)	
O (51)	4c	1497(3)	95(5)	1462(7)	39(4)	
O (52)	4c	1505(3)	5116(5)	1542(6)	43(3)	
O (53)	4c	3551(4)	−45(5)	3695(8)	85(5)	
O (54)	4c	3496(4)	4963(5)	3650(8)	111(5)	
O (55)	4c	3942(4)	2426(5)	1286(7)	68(5)	
O (56)	4c	4010(5)	7596(5)	1370(8)	97(7)	
O (57)	4c	1030(4)	2580(5)	3525(6)	70(4)	
O (58)	4c	973(4)	7631(5)	3432(7)	52(4)	
O (61)	4c	5323(3)	−427(6)	1709(5)	32(3)	
O (62)	4c	5310(3)	4266(4)	1854(6)	18(3)	
O (63)	4c	4658(3)	4571(7)	3264(6)	72(5)	
O (64)	4c	4676(3)	−754(5)	3111(6)	20(3)	
O (65)	4c	2820(3)	1927(6)	1799(7)	85(6)	
O (66)	4c	2867(3)	6836(7)	1873(7)	89(6)	
O (67)	4c	2197(3)	1968(6)	3272(6)	42(4)	
O (68)	4c	2144(3)	6854(6)	3171(7)	53(4)	
O (1W1)	4c	5251(7)	7411(14)	1572(11)	93(7)	1.00(2)
O (1W2)	4c	5218(11)	2150(2)	2060(2)	122(12)	0.69(2)
O (1W3)	4c	4767(7)	2694(14)	3470(11)	99(7)	1.00(2)
O (1W4)	4c	4780(3)	7950(5)	3440(3)	220(7)	0.22(3)
O (1W5)	4c	2757(9)	10270(3)	1580(17)	119(14)	0.52(3)
O (1W6)	4c	2628(15)	5190(4)	1261(19)	150(2)	0.45(3)
O (1W7)	4c	2232(8)	9800(2)	3347(15)	128(9)	0.93(3)
O (1W8)	4c	2268(9)	4784(18)	3442(16)	121(9)	0.96(3)

An intensity analysis from the SMART data set as well as from *Weissenberg* photographs showed that reflections with even *h*,*k*, and *l* were systematically strong, whereas reflections with at least one odd index were very weak. Therefore, a determination of the approximate structure could be carried out using a monoclinic sub-cell, space group C121, with halved *a*, *b*, and *c* lattice constants ($a = 12.089$, $b = 6.903$, $c = 6.354$ Å, $\beta = 90.09°$, refined by the *Rietveld* method from a powder pattern). The structure determination including refinement was carried out be SHELX97 [18]. Resulting atomic parameters of the sub-structure are listed in Table 3.

The structure determined this way is an artificial one which results from a superposition of the real structure with structures shifted in *x*, *y*, and *z* direction by 0.5 a_0, 0.5 b_0, and 0.5 c_0, respectively. The subsequent determination of atomic positions and occupation factors of the super-structure was a complicated task because information about the deviation of the sub-cell symmetry exists only in the systematically weak reflections (*h*, *k*, or *l* odd). Anisotropic displacement parameters of the water oxygen in the sub-cell indicated a splitting in two positions. This was used as starting point for a long refinement procedure for atomic coordinates and occupation factors of Ca, Na, and water. Because of strong correlations between structural parameters and in order to avoid a ‚blow-up' at the beginning of the refinement, large damping factors and several restraints for bond lengths and occupation factors of Ca and Na were introduced. After some hundred refinement cycles a sufficient convergence was achieved; the resulting parameters are given in Table 5[1]. The relatively high *R* value ($R_1 = \Sigma(|F_o|-|F_c|)/\Sigma|F_o|$) of 0.1387 may be explained by the fact that seven eights of the reflection intensities are systematically very weak. This leads to a small denominator $\Sigma|F_o|$, and therefore a higher *R* value is to be expected compared to that of a 'normal' structure for statistical reasons. Furthermore, the crystal used for the structure determination was twinned with (100) as twinning plane. This was taken into account in the structure refinement. The refinement indicated relative volumina of 72 and 28% for both parts of the twin. Structure determinations and refinements from two non-twinned crystals gave similar structural parameters, but the quality of the intensity data sets were somewhat worse compared with that of the twinned crystal. The calculated densities of 2.734 (Table 2) and 2.737 (Table 4) are reasonable compared with a value of 2.757 g/cm^3 reported usually for the α-form of sodium-free hemihydrate.

Acknowledgements

We are grateful for financial support from the *German Ministry of Education, Technology, and Research (BMBF)* as well as from the *Deutsche Forschungsgemeinschaft* (GRK 208/2).

References

[1] Freyer D, Fischer S, Köhnke K, Voigt W (1997) Solid State Ionics **96**: 29
[2] Freyer D, Voigt W, Köhnke K (1998) Eur J Solid State Inorg Chem **35**: 595
[3] Hill AE, Will JH (1938) J Am Chem Soc **60**: 1647
[4] Lepeshkov IN, Fradkina KB (1959) Russ J Inorg Chem **4**(12): 1297
[5] Rassonskaya IS, Semendyaeva NK (1961) Russ J Inorg Chem **6**(8): 891
[6] Rogosowskaya MS, Konontschuk TI, Lukjanowa NK (1980) Zh Neorg Khim **25**: 1095
[7] Reisdorf K, Abriel W (1987) N Jb Min Abh **157**: 44
[8] Powell DA (1962) Austr J Chem **15**: 868
[9] Lager GA, Armbruster T, Rotella FJ, Jorgensen JD, Hinks DG (1984) Am Min **69**: 910

[1] Additional material to this paper can be ordered referring to CSD-410748, names of the authors, and citations of the paper at the Fachinformationszentrum Karlsruhe, Gesellschaft für wissenschaftlich-technische Information mbH, D-76344 Eggenstein-Leopoldshafen, Germany. The list of F_o/F_c data is available from the author up to one year after the publication has appeared.

[10] Bezou C, Christensen AN, Lehmann M, Nonat A (1991) CR Hebd Seances Acad Sci **312**: 43
[11] Kuntze RA (1965) Can J Chem **43**: 2522
[12] Hamad SELD (1981) Trans J Br Cera Soc **80**: 56
[13] Krönert W, Haubert P (1975) TIZ (10) **99**: 238
[14] Lehmann H, Rieke K (1973) TIZ **97**(6): 157
[15] Clifton JR (1972) J Res **76A**(1): 41
[16] Powell DA (1958) Nature **182**: 792
[17] Budnikov PO, Kosyreva ZS (1953) Voprosy Petrografi Minera Akad Nauk SSSR **2**: 342; 1954 Chem Abstr **48**: 13314a
[18] Sheldrick GM (1997) SHELX-97. Universität Göttingen, Germany

Received May 6, 1999. Accepted May 26, 1999